INTERNATIONAL JOURNAL OF MARITIME TECHNOLOGY
IJMT Vol.20 / Summer & Autumn 2024 (13-25)
Available online at: www. ijmt.ir

Effect of Hydrofoil Stabilizer Location on Porpoising of Mono-Hull Planing Craft

Mohsen Saeedi Namini[1], Ahmadreza Kohansal[2*]

[1] *M.Sc. Student, Persian Gulf University; Mohsen.saeedinamini@gmail.com*
[2] *Assistant Professor, Department of Marine Engineering, Persian Gulf University; kohansal@pgu.ac.ir*

ARTICLE INFO

Article History:
Received: 28 Jan 2024
Accepted: 8 Jun 2024
Available online: 10 Jun 2024

Keywords:
Porpoising
Planing craft
Mono-Hull
Hydrofoil Stabilizer
Dynamic Motions

ABSTRACT

In this study, the effect of hydrofoil stabilizer location on the porpoising instability of a mono-hull planing craft and also its optimal location have been investigated. The craft used in this project was a planing mono-hull one which was longitudinally unstable in the sea test. More precisely, it should be said that the craft entered the longitudinal instability stage at a speed of 30 knots and severe changes in its pitch and heave movements were observed. Numerical simulation which was based on computational fluid dynamics (CFD) techniques was done to simulate a three-dimensional geometric model in the fluid Eulerian two phases flow. A validation study was carried out by comparing the numerical results with the experimental data of the planing hull without the hydrofoil stabilizer. To study the effect of the installation position of the hydrofoil stabilizer, three parameters include depth of the hydrofoil relative to the transom bottom, the longitudinal distance of hydrofoil from the transom and the angle of attack were selected. The effects of changes in each of these parameters were investigated separately. Finally, the most suitable installation parameters that provide the best performance of the hydrofoil stabilizer and reduce the porpoising influence were selected. From the results of this study, it was observed that by increasing the depth of the hydrofoil from the transom and also by increasing the angle of attack of the hydrofoil, the amplitude of heave and pitch diagrams has decreased. The longitudinal distance of the hydrofoil to transom has not significant effect on porpoising instability. However, the results showed that the proper position for the hydrofoil stabilizer should not be under the hull bottom.

1.Introduction

A planing craft is a type of high-speed boat that, when it moves at a sufficient speed, most of its weight is supported by the lifting forces acting on its bottom [1]. Stability problems of high-speed crafts are very important even in calm waters. The trim variations may create the instabilities such as porpoising [2]. Porpoising is a hull's heave and pitch, coupling oscillation with sustained or increasing amplitudes [3]. During porpoising, the vessel's bow jumps up and down out of the water, even in calm waters due to change in the center of pressure of bottom [4].

This drastically motion can result in structural damage in craft hull. In addition, it can be mentioned that the occurrence of porpoising can have other effects such as accidents and unsafe conditions of vessels and can also cause discomfort to the crew. Therefore, porpoise prevention is very important and it is vital that it is considered during the design phase of the planing craft. However, sometimes after the construction of a vessel and during the test phase at sea, it is determined that the vessel has porposing instability. In this situation, several methods have been proposed to fix or reduce these instabilities.

Some suggested solutions to eliminate or reduce porpoising instability of the craft include reducing the trim angle, shifting the center of gravity and using the trim tab. In addition, methods such as reduction of speed, increasing the angle of deadrise and reducing the aspect ratio of hull can also be used in certain situations. It is not possible to use these methods in all cases, and choosing the right method to fix or reduce instabilities depends on many factors.

Hydrofoil stabilizers are one of the low-cost methods to reduce porpoising without changing the structure of the craft hull. The hydrofoil stabilizer is a special type of hydrofoil which can be attached to the cavitation plate or plates of an outboard motor or a stern drive. Its structure and function are significantly similar to the trim tab.

The hydrofoil stabilizer has a low construction and maintenance cost and at the same time it can be easily installed. Also, this type of hydrofoil stabilizers is known as “Whale tail”, “Doel-fins” and “Stingray”.

Perhaps the first attempt to make this form of plates was invented by Don W. King et al. which was called “Anti-cavitation plate for outboard motors” [5], then it was invented by Larson to reduce the instability of the boat [6].

Different research studies have been conducted on the performance and behavior of planing hulls. It can be said that the only systematic experimental investigation of porpoising for prismatic planing boats was carried out by Day and Haag [7]. Their results showed that, the porpoising limits can be expressed in terms of the trim angle and the lift force coefficient for different deadrise angles. Also, the first important study of planing phenomenon took place in Davison Laboratory at Steven institute of technology by Savitsky [8]. This study resulted in several technical reports, including definition of planing surface lift, wetted area, pressure distribution, wake shape and etc. Savitsky also presented porpoising experimental limits for the prismatic body [7].

Clement and Blount [9] performed a series of hydrodynamic experiments based on the two different models with different deadrise angles to obtain the resistance performance of the models. Several other studies were conducted like experimental and theoretical study of Brown [10] on planing surfaces with trim tabs. Few years later, another paper was published by Savitsky and Brown [11] in which effects of controlling the trim tabs was studied. From that time on, the study of trim tabs became more popular and their usage in controlling the additional trim of planing hulls became the focal point of other studies. Blount and codega [12] conducted studies about dynamic stability of planing boats. They reported data for boats exhibiting non-oscillatory dynamic instability. They suggest quantitative criteria which may result in development of dynamically stable planing boats. Analyses of the hydrodynamics of the Cougar high-speed vessel, a hard chine planing hull was done by Kazemi and Salari [13]. Their study was about the effects of different parameters on the hydrodynamic characteristics of the planing craft. Xiaosheng Bi et al. [14] analyzed the hydrodynamic performance of a planing craft with a fixed hydrofoil in regular waves. Numerical simulations are carried out to study the hydrodynamic performance of the planing craft and the influence of the fixed hydrofoil on its seakeeping. Zan et al. [15] studied experimentally on porpoising of high-speed planing trimaran that led to the prediction of porposing of this craft.

Considering the advantages of using hydrodynamic stabilizers and also the lack of published research results in this field, therefore, in this research, with a CFD solver, the simulation of the hydrofoil stabilizer and its impact on the porpoising have been investigated.

The present study mainly includes four aspects. At first, the computational domain and boundary conditions of the problem are determined and the three-dimensional modeling of the mono-hull planing craft and hydrofoil stabilizer is performed. In the third step, the numerical simulation of motions of planing craft is done. Modeling of the hydrofoil stabilizer, analyzing the effect of its use on the porpoising of the planing craft, as well as the effect of its installation position, are among the most important tasks that are carried out in the fourth step. The numerical method is entirely based on implicit unsteady in conjunction with DBFI and overset mesh to improve the precision and efficiency of the numerical simulation.

A validation study is carried out by comparing the numerical results with the various experimental results. The conditions of the simulated model are the same as the experimental model, and both models enter the stage of longitudinal instability at approximately the same speed. In this study, other parameters such as depth from the transom bottom, the longitudinal distance to the transom and the angle of attack of hydrofoil stabilizer have been investigated.

2.Model Geometry Specifications

At the first step, a 3D model of a mono-hull planing craft was prepared in a CAD software. The basic specifications for the hull are shown in Table 1. Also, a 3D model of the planing craft and its body lines are shown in Figure 1 and 2, respectively. In fact, it is a simplified form of the original mono-hull craft. The simplifications included removing the motor, propeller, passenger areas, and then simplifying top of hull with flat geometry. These simplifications are done to increase the accuracy and reduce the computation time.

Table 1. Main Dimensions of base craft

Characteristic	Value
Length	5000 [*mm*]
Width	1940 [*mm*]
Height	740 [*mm*]
Mass	1000 [*kg*]
Speed	30 [knot]
Engine	300 [hp]
Longitudinal center of gravity	1750 from transom [mm]

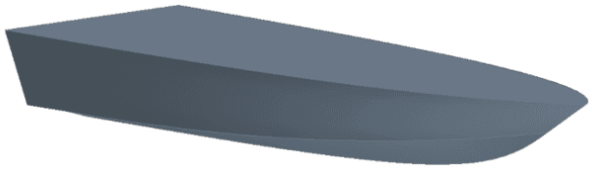

Figure 1. A 3D model of mono-hull planinig craft

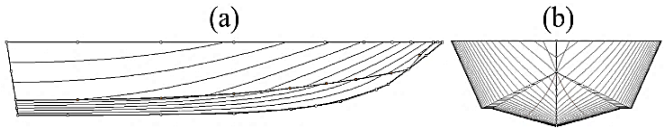

Figure 2. Mono-hull body lines;
(a): Right view, (b): Front view

The hydrofoil stabilizer described in this paper is modeled in a simple form, has shown in Figures 3 and 4. Geometrical parameters of simple form of hydrofoil as shown in Table 2 are length, width and thickness.

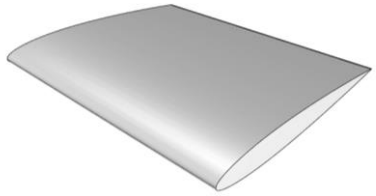

Figure 3. 3D model of simple form of hydrofoil stabilizer

In order to investigate the effect of the hydrofoil stabilizer in simulation, first, a hydrofoil with a standard NACA 0012 [16] is considered. The two-dimensional section of this hydrofoil has shown in Figure 4.

Based on the existing models, according to the power of the motorcraft, which is 300 horsepower, the dimensions of the hydrofoil are assumed to be 40 cm in width and 30 cm in chord length [17]. Also, based on the standard type of hydrofoil, the thickness of the hydrofoil is considered to be 4.3 cm (Table 2).

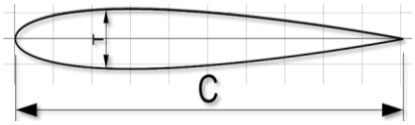

Figure 4. Parameters of simple hydrofoil stabilizer [16]

Table 2. Dimensions of hydrofoil stabilizer

Characteristic	Value
C (Chord length)	30 [*cm*]
B (Maximum width)	40 [*cm*]
T (Maximum thickness)	4.3 [cm]

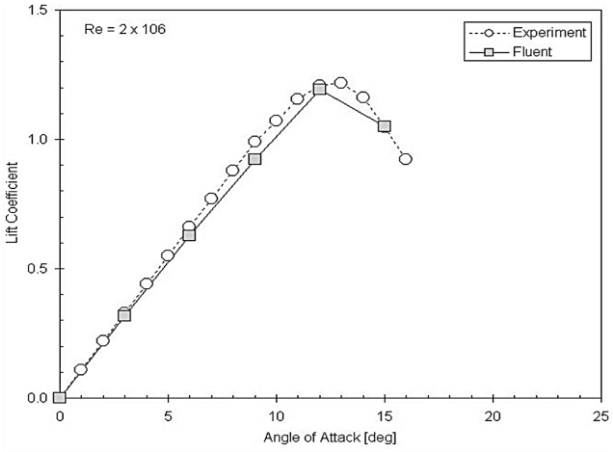

Figure 5. Lift coefficient−angle of attack diagram [18]

According to the angle of attack shown in the NACA-0012 [16] standard in Figure 5, it is determined that the maximum angle of attack that can be used for the hydrofoil is equal to 12 degrees. Therefore, research was conducted in three attack angles of 0, 5 and 10 degrees.

Combination of two geometries, which shows a hydrofoil stabilizer at the rear of the craft transom is shown in Figure 6. The parameters that are investigated in this article are stated in Table 3 and are shown in Figure 7.

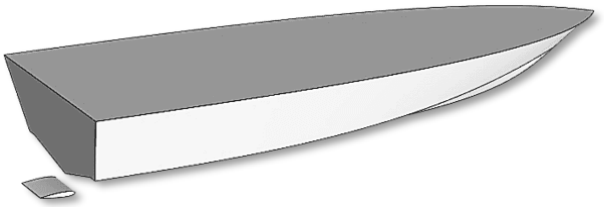

Figure 6. Combination of two models, perspective view

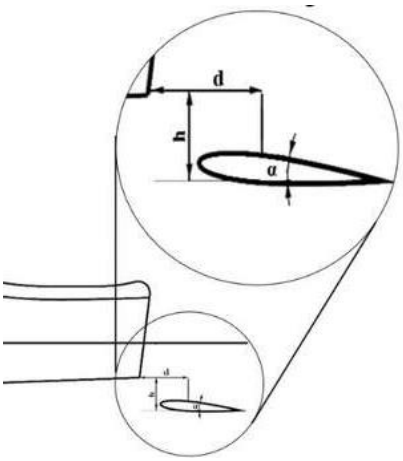

Figure 7. Location parameters of hydrofoil stabilizer

Table 3. Positional parameters of hydrofoil stabilizer

Parameter	Description
H	Depth from the transom bottom
D	Longitudinal distance from the transom
α	Angle of attack

3.Governing Equations

Numerical simulation which was based on computational fluid dynamics (CFD) techniques was done to simulate a three-dimensional geometric model in the fluid Eulerian two phases flow. The method was entirely based on Reynolds-Averaged Navier-Stokes (RANS) equations, moreover, the volume of fraction (VOF) scheme was used to model the free surfaces. The standard K-ε turbulent model and the overset mesh technique in conjunction with DBFI were implemented

to improve the precision and efficiency of the numerical simulation. Continuity and RANS equations can be written as:

$$\frac{\partial \bar{u}_i}{\partial x_i} = 0 \qquad (1)$$

$$\frac{\partial(\bar{u}_i)}{\partial t} + \bar{u}_j \frac{\partial(\bar{u}_i)}{\partial x_j} = -\frac{1}{\rho}\frac{\partial \bar{p}}{\partial x_i} + \frac{\partial}{\partial x_j}\left[\nu\left(\frac{\partial \bar{u}_i}{\partial x_j} + \frac{\partial \bar{u}_j}{\partial x_i}\right)\right] - \frac{\partial \overline{\acute{u}_\iota \acute{u}_j}}{\partial x_j} \qquad (2)$$

where p is the pressure, ρ is the fluid density, ν is the kinematic viscosity, $\bar{u}_i$ and $\bar{u}_j$ depict average velocity components while $\acute{u}_\iota$ and $\acute{u}_j$ represent fluctuating components in i[th] and j[th] direction. The combination of k and ε defines turbulent eddy viscosity μ_t, as follows:

$$\mu_t = C_\mu \frac{k^2}{\varepsilon} \qquad (3)$$

Where C_μ is constant and it depends on both the mean flow and turbulence properties. k is the turbulent kinetic energy, ε is the dissipation rate of k and both of them calculatable from Transport Equations are given as follows:

$$\frac{\partial k}{\partial t} + \frac{\partial(kU_j)}{\partial x_j} = \frac{\partial}{\partial x_j}\left[\left(\nu + \frac{\nu_t}{\sigma_k}\right)\frac{\partial k}{\partial x_j}\right] + P_k - \varepsilon \qquad (4)$$

$$\frac{\partial \varepsilon}{\partial t} + \frac{\partial(\varepsilon U_j)}{\partial x_j} = \frac{\partial}{\partial x_j}\left[\left(\nu + \frac{\nu_t}{\sigma_\varepsilon}\right)\frac{\partial \varepsilon}{\partial x_j}\right] + C_{\varepsilon 1} P_k \frac{\varepsilon}{k} - C_{\varepsilon 2}\frac{\varepsilon^2}{k} \qquad (5)$$

where σ_k, σ_ε, $C_{\varepsilon 1}$, $C_{\varepsilon 2}$ and C_μ are model constants and P_k is the production of turbulent kinetic energy. A production limiter is used to avoid the build-up of turbulence, that defined as:

$$P_k = -\overline{u_\iota u_j}\frac{\partial \overline{U_\iota}}{\partial x_j} \qquad (6)$$

4.Numerical Simulation

The computational domain is a hypothetical towing tank in the simulation software, which is also called the far field. The computational domain has shown in Figure 8. In order to have good results, the domain must be far larger than the main model. The dimensions of the computational domain have been determined in a way that the minimum ITTC [18] criteria are considered. The time step on the fine mesh was selected as $\Delta t = 0.005 \sim 0.01 \times \frac{L_w}{U}$, (where L_w is wet length and U is body speed) in accordance with ITTC recommendations.

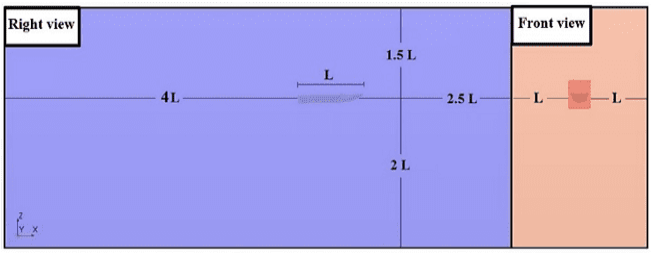

Figure 8. Dimensions of computational domain

The boundary conditions used in the simulation are velocity inlet, pressure outlet, symmetry plan, overset mesh and wall. The front surface of the computational domain is set as a velocity inlet, the back side is a pressure outlet, the top side is symmetry plan, the bottom side and the both sides of the computational domain are walls. Domain and boundary condition are shown in Figures 9.

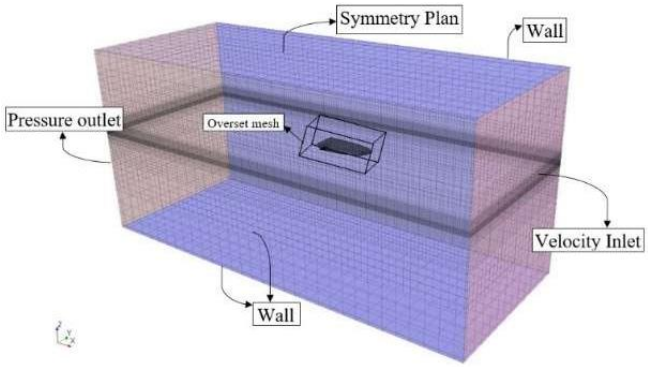

Figure 9. Boundary conditions used in the Simulations

For more accuracy in mesh generation, six volumetric mesh controls were used to refine the meshes. The mesh improvement volumes around of free-surface and hull are shown in Figure 10. The mesh models used in the simulation are surface remesher, trimmer and prism layer mesher. Also, for more accuracy in mesh generation, different mesh volumes with various density are used, which are called mesh improvement volumes. The free-surface mesh improvement volumes are shown in Figures 10.

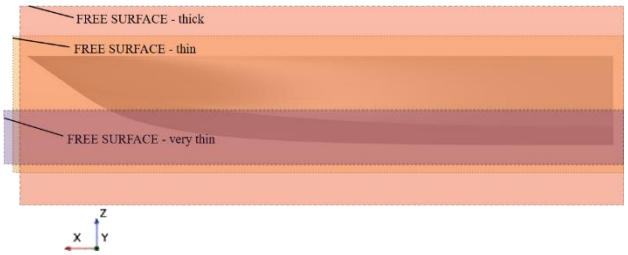

Figure 10. Mesh improvement volumes of free surface

The mesh models used in the simulation are surface remesher, trimmer and prism layer mesher. This prism layers were designed to determine the flow very close to the hull that increased accuracy of meshes around the hull and in the boundary layers. The overset region used when two separate meshes are overlapped and one of them can be move with the moving hull. Also, the

mesh can be translating and rotate. Generated meshes in the computational domain using trimmer method are shown in Figure 11. The specification of moving meshes and stationary meshes are shown in Tables 4 and 5, respectively.

Table 4. Specification of stationary meshes

Node [Property]	Setting
Base Size	0.075 m
Relative Max cell Size [Percentage of Base]	1600
Surface Curvature [# Pts./circle]	36
Surface growth rate	1.3
Relative min Size [Percentage of Base]	6
Relative target Size [Percentage of Base]	40
Template Growth Rate	Slow

Table 5. Specification of moving mesh

Node [Property]	Setting
Base Size	0.05 m
Relative Max cell Size [Percentage of Base]	1600
Surface Curvature [# Pts./circle]	36
Surface growth rate	1.3
Relative min Size [Percentage of Base]	6
Relative target Size [Percentage of Base]	40
Number of Prism Layers	11
Thickness of near wall prism layer	3.0e-4 m
Template Growth Rate	Slow

(a)

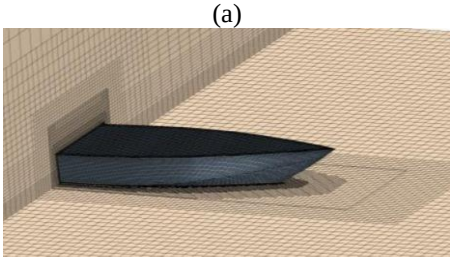

(b)

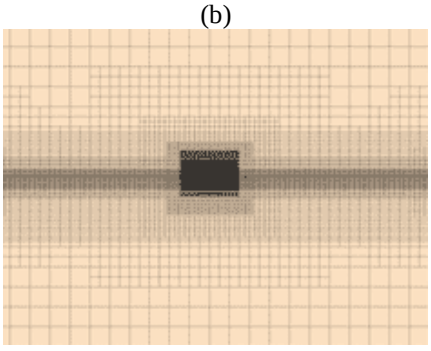

Figure 11. Trimmer meshing of the computational domain; (a): Prespective view, (b): Front view

The mesh model had to be independent and not affect the final results. A mesh dependency study was performed to ensure that the results were independent of the mesh. In order to achieve this goal, four different mesh elements were created to simulate the craft at a speed of 30 knots.

As in figure 12 is shown, there was less than 6% difference between the drag coefficient of first and second points. Therefore, in order to have sufficient accuracy in the calculations and in the shortest possible time, the number of meshes about 2.5 million meshes has been considered as the basic mesh.

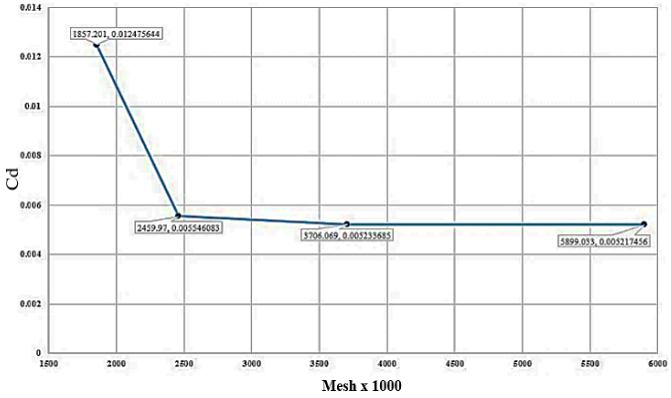

Figure 12. Drag Coefficient-Mesh Graph

The next phase of the study was to verify the numerical results using experimental data. First, to validate the numerical method, a bare planing mono hull craft without the hydrofoil stabilizer was considered. Validation of the numerical calculation was done by comparing the total resistance-speed graph with the results that predicted from experimental methods (Figure 13).

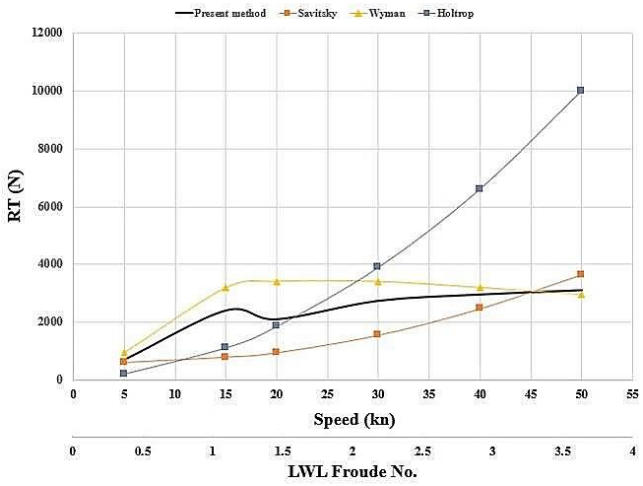

Figure 13. Resistance-speed and Froude number for the planing craft

As it can be observed, by comparing the graphs, generally, there is a reasonable agreement between numerical and experimental results. In other words, it can be said that the numerical method was able to estimate resistance changes with relatively good accuracy.

5.Numerical results

At first, the effect of planing craft speed on porpoising has been investigated. In order to check the longitudinal stability of the planing craft and the starting stage of the porpoisng, the analysis has been done at speeds of 15, 20, 30 and 40 knots. The results related to these simulations and the vessel's pitch and heave motions for each of the mentioned speeds are given in Figures 14, 15, respectively.

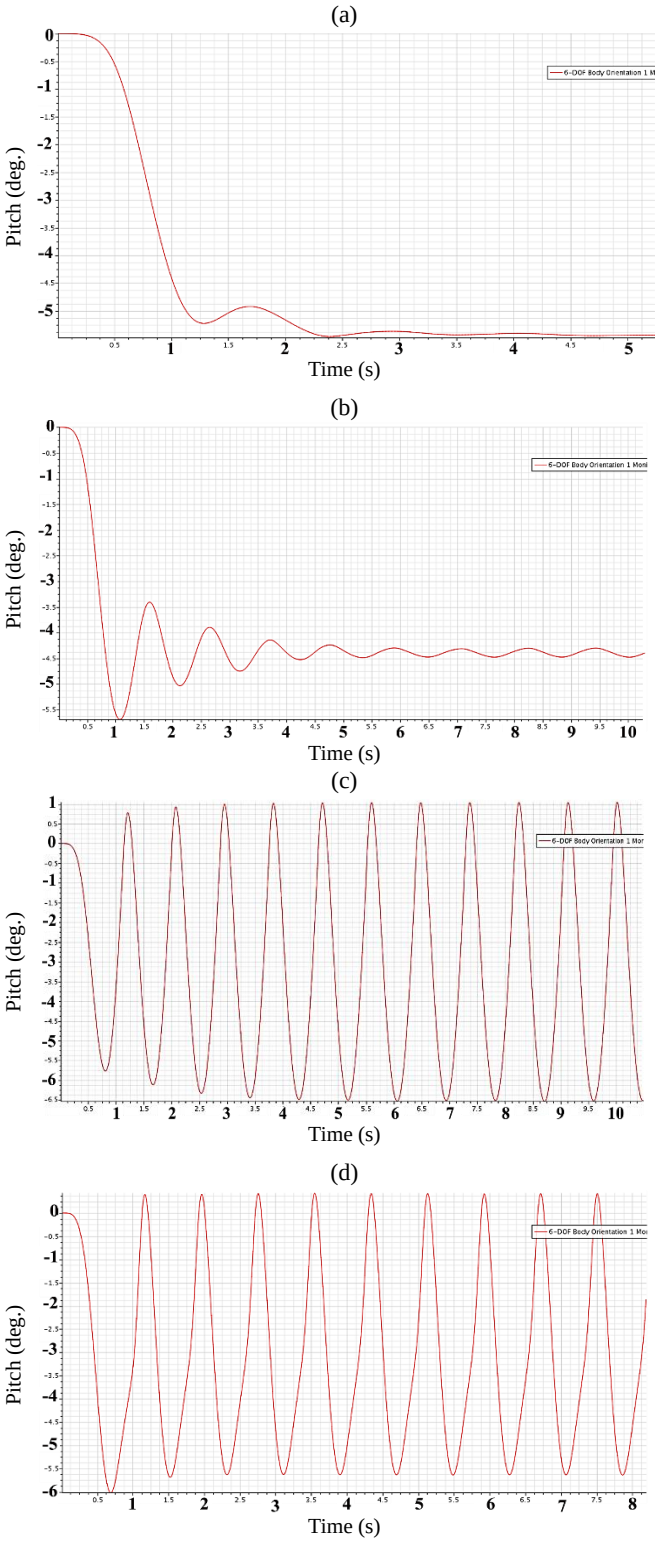

Figure 14. Diagram of Pitch motion at four different speeds; (a): 15 knots, (b): 20 knots, (c): 30 knots, (d): 40 knots

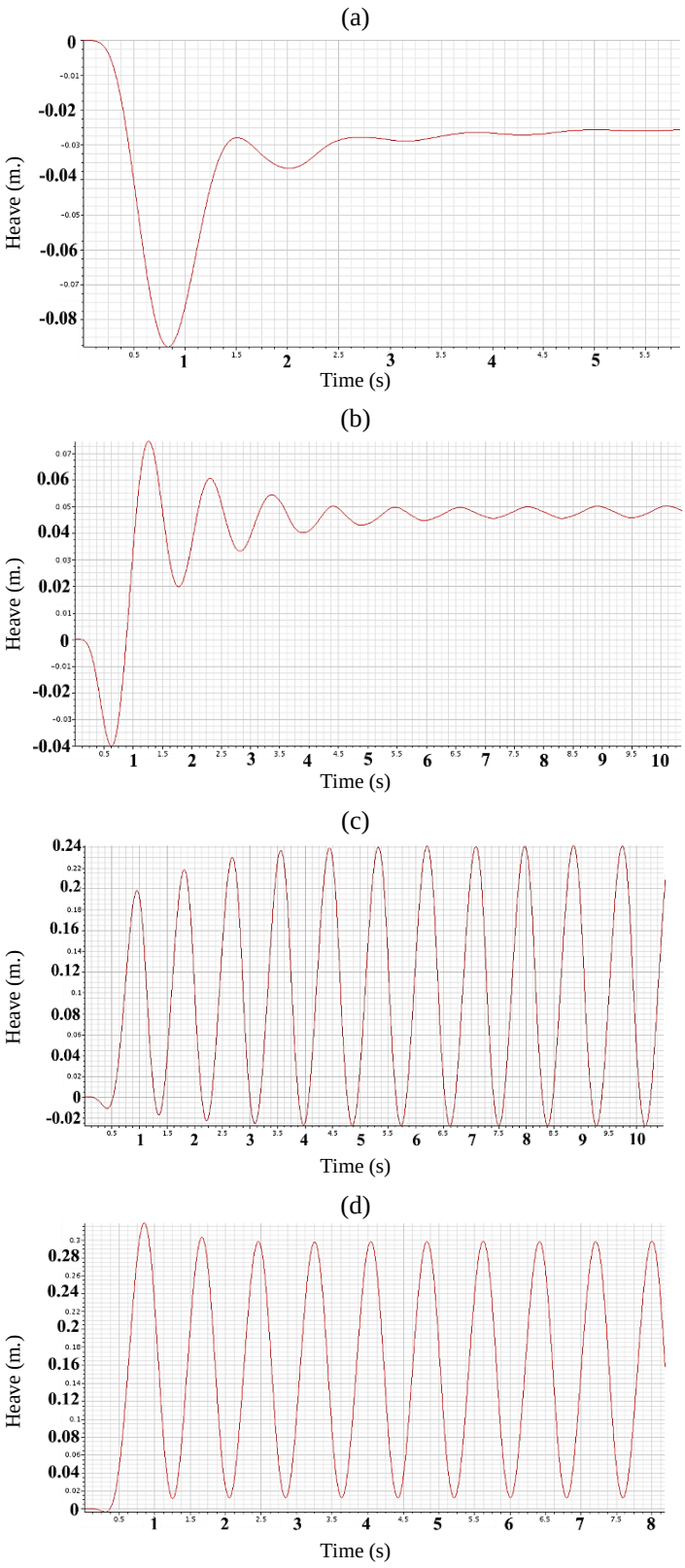

Figure 15. Diagram of Heave motion at four different speeds; (a): 15 knots, (b): 20 knots, (c): 30 knots, (d): 40 knots

As can be seen from Figures 14 and 15, initially, at a speed of 15 knots, the craft is almost stable, but the effects of instability are partially visible in the graphs (Figures 14a and 15a).

As can be seen from Figures 14b and 15b, in this situation, the boat gradually enters the stage of

longitudinal instability and relatively small changes in the angle of pitch and movement of the heave are observed. This situation can be considered as the unstable speed of the craft and the hydrofoil stabilizer can be designed for this speed.

As seen in these two figures, with the increase in speed and reaching the speed of 30 knots, (Figures 14c and 15c) there are many changes in the pitch angle and heave motion. As the speed increases further, these longitudinal instabilities continue. This is completely consistent with what was observed in the floating test with increased speed.

In some cases, by the increase in speed, the craft reaches the longitudinal equilibrium state. The purpose of this part, is to ensure that longitudinal instability continues with increasing speed. As it can be seen from the figures 14(d) and 15(d), the changes of the heave and pitch of the craft are still high and the craft has maintained its unstable state. Therefore, it was observed numerically that the boat has a longitudinal instability of porpoising type after the speed of 30 knots. This result is consistent with the results of the sea trial test report and shows the relative accuracy of the numerical model. In the rest of simulation, effect of parameters changing have investigated in different cases that their scenarios are shown in Table 6.

Table 6. Parameters changing at 30 knots

Study	Cases	H [cm]	D [cm]	α [deg.]
Depth from the transom bottom	Case 1	5	0	0
	Case 2	10	0	0
	Case 3	15	0	0
Longitudinal distance from the transom	Case 4	10	-30	0
	Case 5	10	5	0
	Case 6	10	10	0
	Case 7	10	15	0
Angle of attack	Case 6	10	10	0
	Case 8	10	10	5
	Case 9	10	10	10

In the next step of this study, the effect of the depth of the hydrofoil relative to the bottom of the transom on the behavior of the craft porpoising was investigated. At this point, the hydrofoil was modeled at three depths of 5, 10, and 15 cm from the transom bottom. These three cases are named case1 to case3 in Figure 16. It should be noted that in all these cases, the longitudinal distance of the hydrofoil from the transom is considered to be zero.

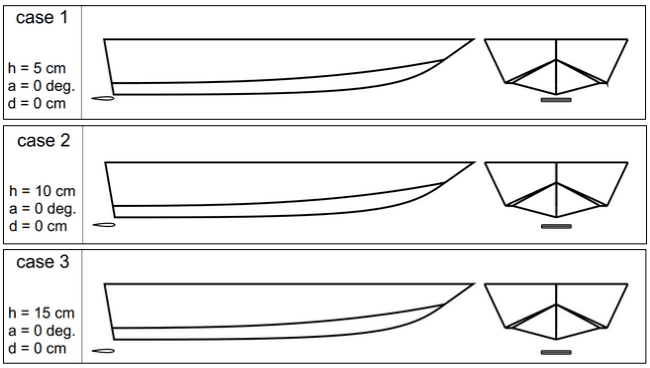

Figure 16. View of the craft with hydrofoil at three depths of 5, 10, and 15 cm from the transom bottom

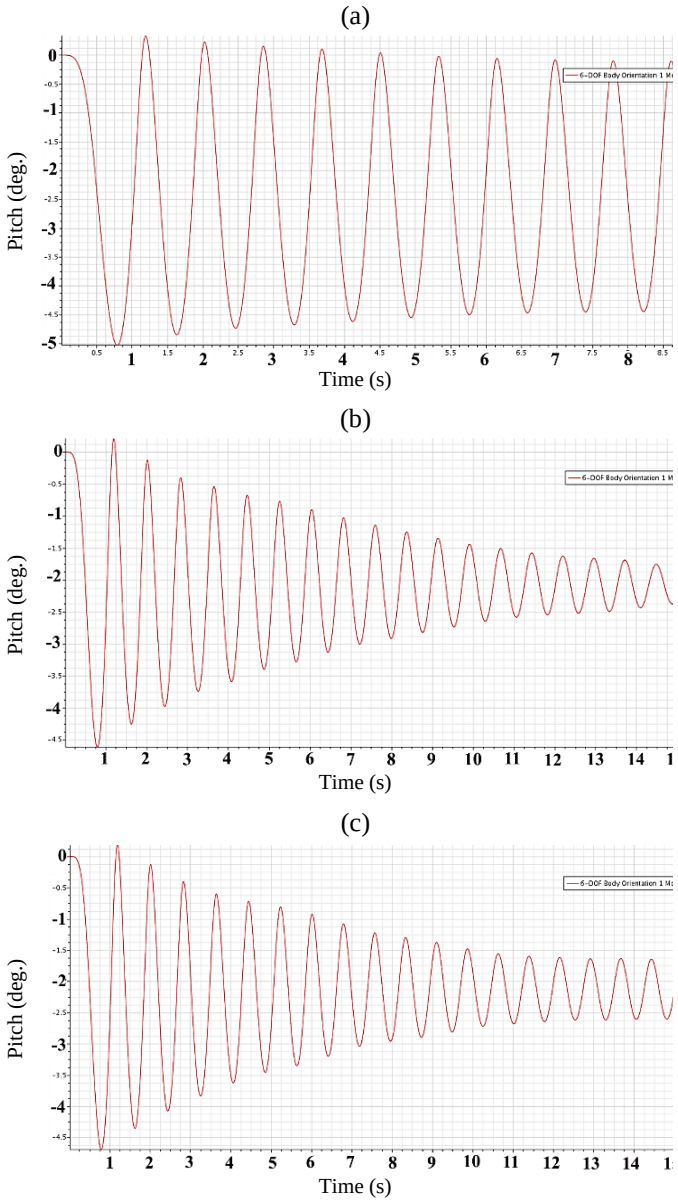

Figure 17. Diagram of Pitch motion in (a): case 1: h = 5 cm, (b) case 2: h = 10 cm and (c) case 3: h = 15 cm

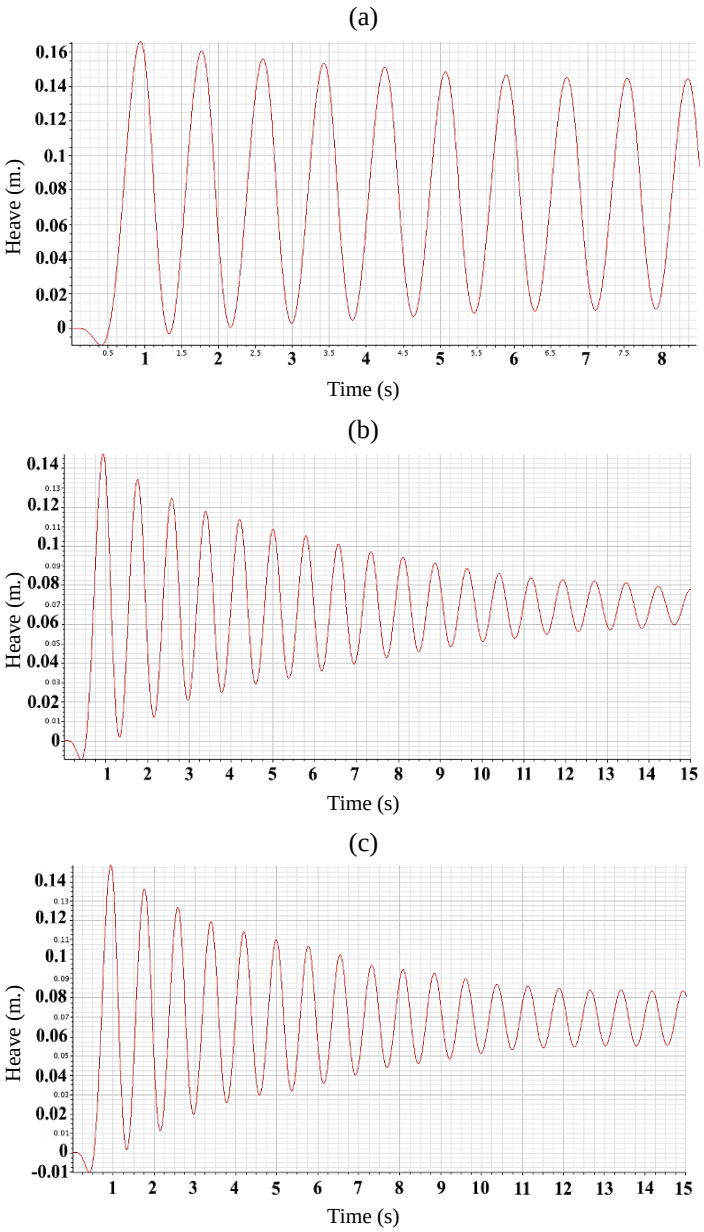

Figure 18. Diagram of Heave motion in (a) case 1: h = 5 cm, (b) case 2: h = 10 cm and (c) case 3: h = 15 cm

The pitch and heave diagrams that have been obtained from the analysis of cases 1-3 are shown in Figures 17 and 18, respectively. As it is clear from this graph, it compares the results of three cases The depth of the hydrofoil to the craft's transom bottom are 5, 10 and 15 cm, respectively.

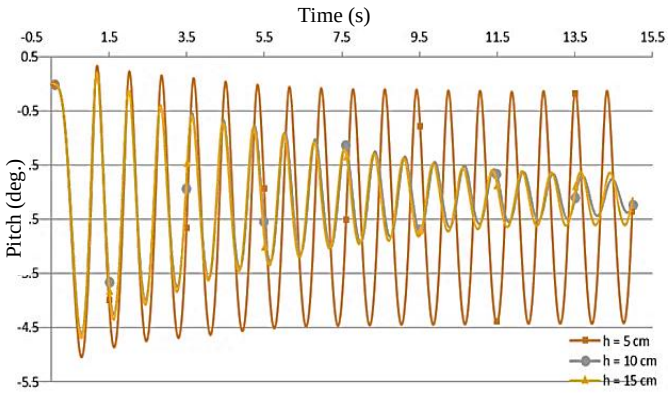

Figure 19. Pitch-time diagram of cases 1 to 3

It can be seen that by increasing the depth of the hydrofoil from the bottom of the craft, the longitudinal instability has reduced and the craft reaches the longitudinal stability state faster. However, the small difference in the graphs between the depths of 10 and 15 cm shows that increasing in depth causes a decrease in the longitudinal instability in a non-linear way, and further increase of hydrofoil

l depth has no effect on reducing instability. In other word, the higher depth of the hydrofoil from the bottom does not make much difference in eliminating the instability. Therefore, in this analysis, the hydrofoil stabilizer has the best performance at a depth of 10 cm from the transom bottom and other parameters are examined at this depth (Fig. 19).

The effect of the longitudinal distance of the hydrofoil to the transom on porpoising instability was another issue that was studied in this research. In order to investigate the effect of the longitudinal distance of the hydrofoil to the transom of the craft, modeling of the hydrofoil was done in four cases (cases 4-7), as shown in the Figure 20. First, the best depth was selected and then the longitudinal distances of the hydrofoil at the mentioned depth were analyzed.

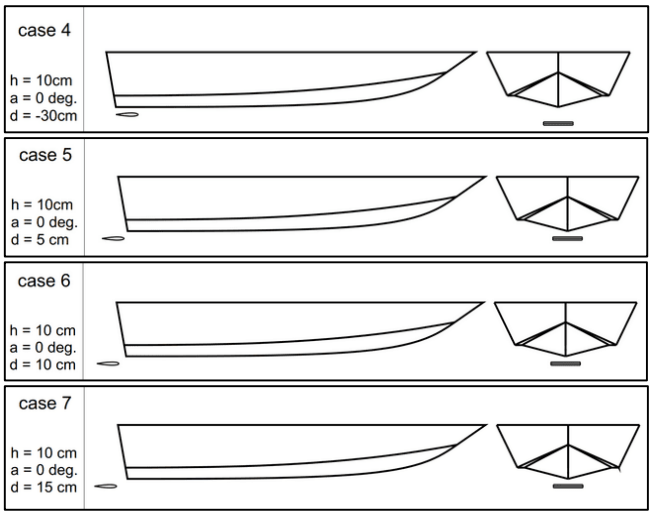

Figure 20. View of the craft with hydrofoil in three different longitudinal distances case 4: d = -30 cm, case 5: d = 5 cm and case 6: d =10 cm from transom bottom

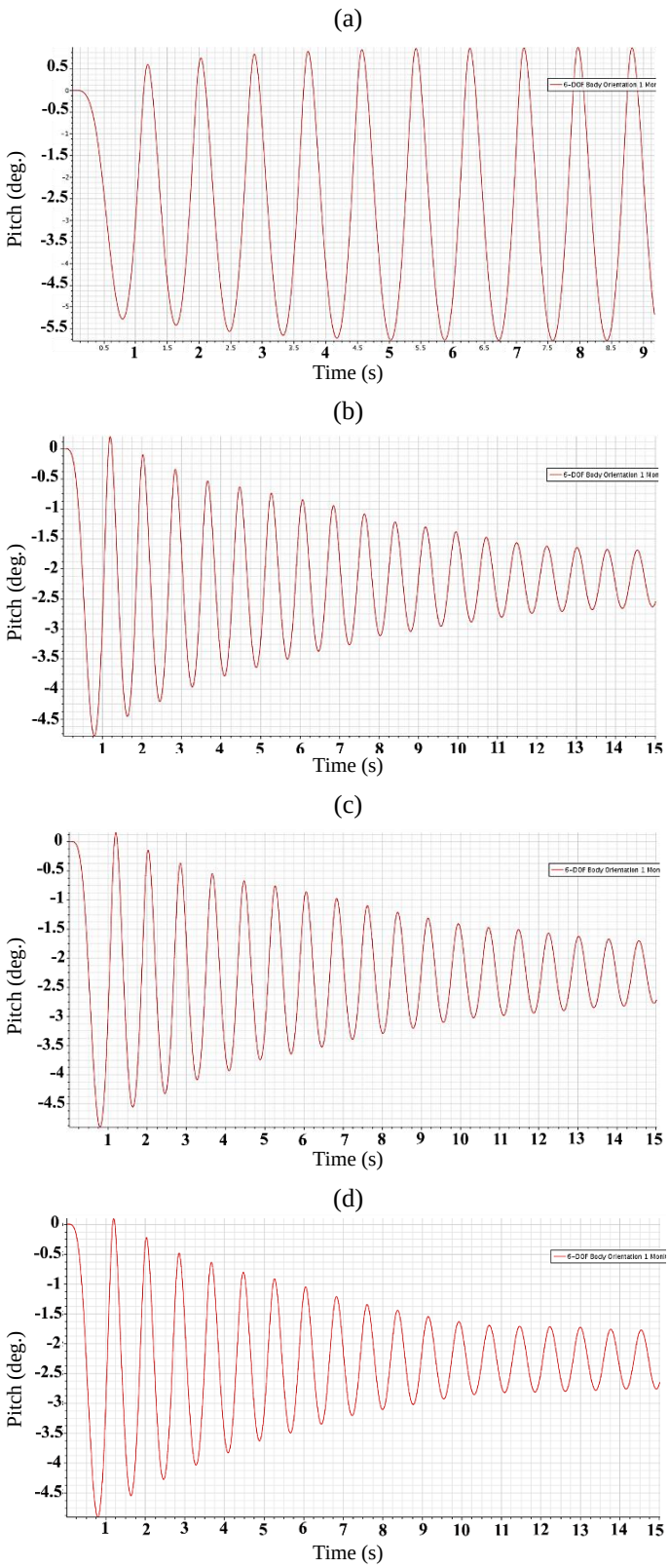

Figure 21. Diagram of Pitch motion in four different longitudinal distances;
(a) case 4: d = -30 cm, (b) case 5: d = 5 cm, (c) case 6: d =10 cm and (d) case 7: d=15 cm from transom bottom

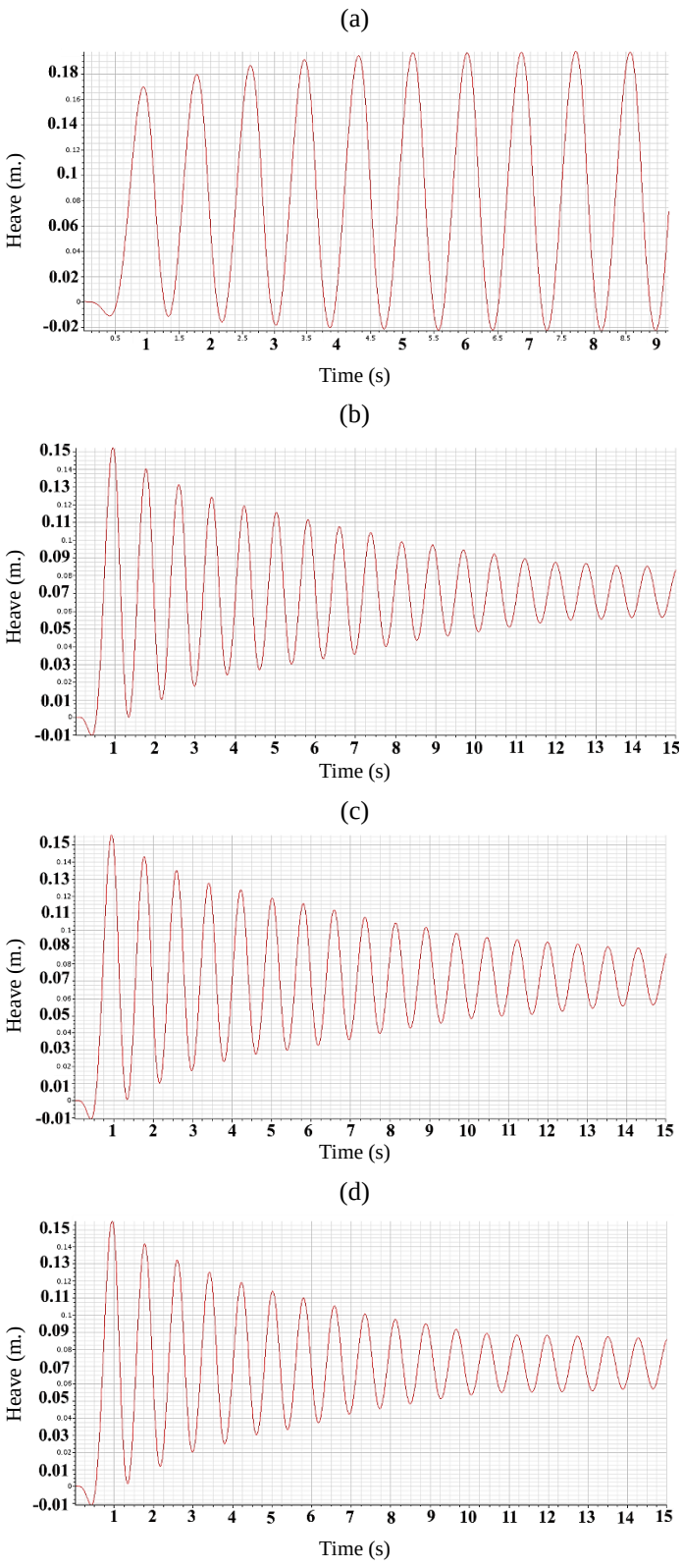

Figure 22. Diagram of heave motion in four different longitudinal distances;
(a) case 4: d = -30 cm, (b) case 5: d = 5 cm, (c) case 6: d =10 cm and (d) case 7: d=15 cm from transom bottom

By analyzing the diagrams of case 4, the longitudinal position of the hydrofoil under the transom of hull has no effect on reducing the longitudinal instability of the craft, and as it has been determined from the subsequent analysis, the proper position for the hydrofoil should be after the transom of the craft.

The pitch and heave time diagram are obtained from the analysis of cases 4-7 and has been showed in Figures 21 and 22. The longitudinal distances of the hydrofoil from the transom of the craft are 5, 10 and 15 cm, respectively. It should be considered that the height of the hydrofoil from the transom bottom is equal to zero. Also, the angle of attack in these four cases were assumed to be zero.

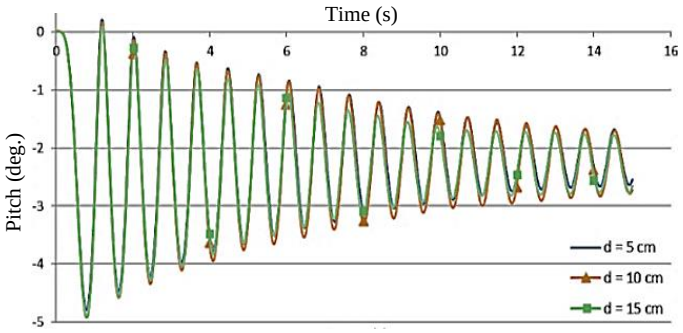

Figure 23. Pitch-time diagram of cases 4-7

As it is clear from Figure 23, by comparing the results of the three cases, it can be seen that by increasing in the longitudinal distance of the hydrofoil from the transom is an effective parameter in reducing the longitudinal instability. However, there are small differences in the diagram between the longitudinal distances. Therefore, in this analysis, the dimensions of engine and propeller determine the longitudinal position of the hydrofoil stabilizer. To examine other parameters, the longitudinal distance of the hydrofoil stabilizer from the transom is assumed to be 10 cm.

Finally, the Effect of the attack angle of the hydrofoil on porpoising has been investigated. According to the figure 2 (lift coefficient-attack angle diagram), it is found that the maximum angle of attack for the hydrofoil is 12 degrees and it should be considered that the angle of attack is less than the stall angle. Therefore, this research has been done in three angles of attack, that are equal to 0, 5 and 10 degrees.

In these three cases (cases 6, 8, 9), the hydrofoil was modeled in three angles of attack 0, 5 and 10 degrees, and the height of the hydrofoil from the bottom of the transom bottom is considered constant and equal to 10 cm, and also the longitudinal distance of the hydrofoil from the transom is considered equal to 10 cm (Fig. 24).

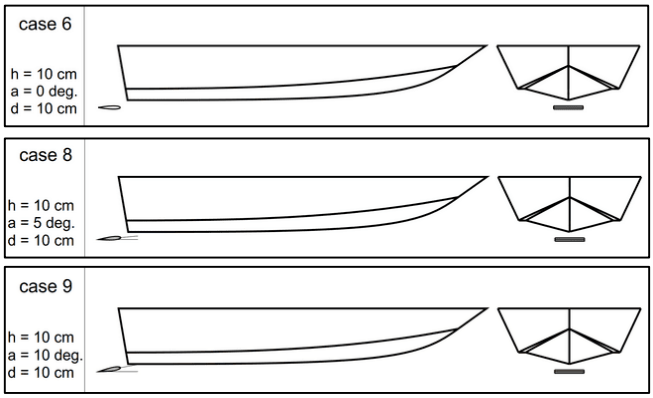

Figure 24. View of the craft with hydrofoil in cases 6, 8 and 9

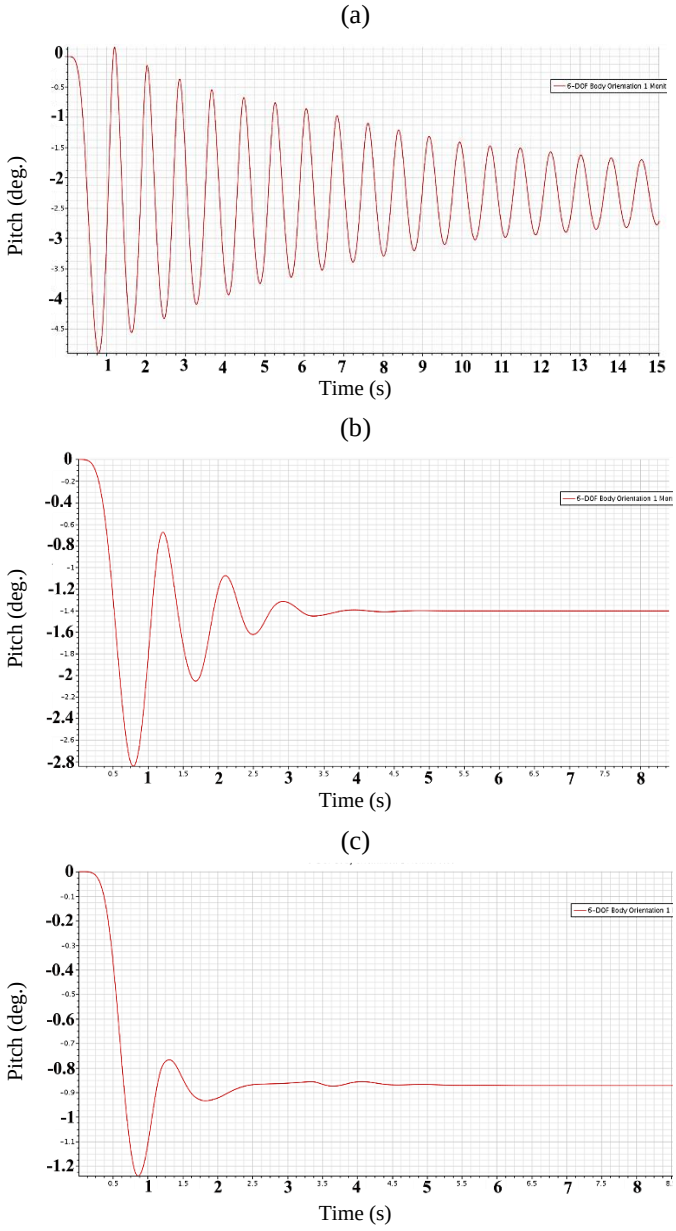

Figure 25. Diagram of Pitch motion in three different angles of attack;
(a) case 6: α = 0 deg, (b) case 8: α = 5 deg, (c) case 9: α = 10 deg

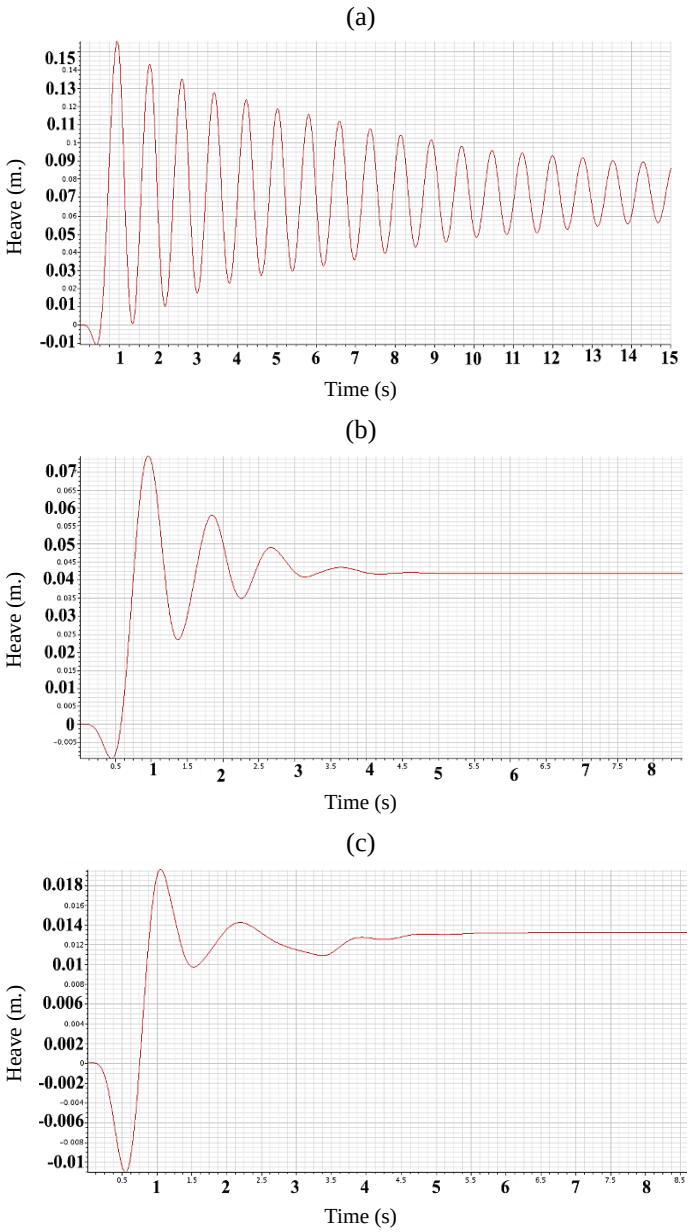

Figure 26. Diagram of Heave motion in three different angles of attack;
(a) case 6: α = 0 deg, (b) case 8: α = 5 deg, (c) case 9: α = 10 deg

The pitch and heave time diagram is obtained from the analysis of cases 6, 8, 9 and has been shown in Figures 25 and 26. The attack angles of the hydrofoil stabilizer are 0, 5 and 10 degrees, respectively. As it mentioned, that the angle of attack is less than the stall angle.

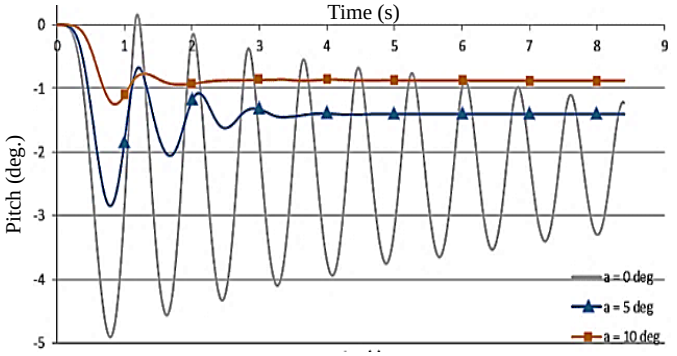

Figure 27. Pitch-time diagram of cases 6, 8 and 9

As it is clear from Figure 27 that it compares the results of three cases, the increasing the angle of attack of the hydrofoil has a significant effect in reducing the longitudinal instability and the craft reaches the stability state faster than other parameters. The reason for the increase in longitudinal stability is the increase in the hydrofoil lift to drag ratio, which generated a large lift force at the bottom of the craft and finally it reduced the dynamic trim of the craft. Therefore, according to this diagram, the attack angle of 10 degrees was chosen as the best case between cases 6, 8 and 9.

In Table 7, a comparison has been made between the amplitude values of pitch and heave motions of the boat without and with hydrofoil stabilizer based on the cases shown in Table 6 (cases 1 to 9). This comparison was made at a speed of 30 knots and in a time of 3 seconds. In this condition, the amplitude values of pitch and heave motions of the boat without hydrofoil stabilizer are 3.75 degrees and 0.13 meters, respectively.

Table 7. Comparison of the amplitude values of heave and pitch motions at 30 knots & in 3 seconds

Case	Pitch [deg.]	Heave [m]	Diff.%	
			Pitch%	Heave%
Case 1	2.375	0.078	36.67	40.38
Case 2	1.625	0.05	56.67	61.54
Case 3	1.625	0.05	56.67	61.54
Case 4	3.25	0.105	13.33	19.23
Case 5	1.75	0.053	53.33	59.62
Case 6	1.75	0.055	53.33	57.69
Case 7	1.875	0.053	50.00	59.62
Case 8	0.1	0.05	97.33	61.54
Case 9	0.063	0.002	98.33	98.46

For selected cases, as can be seen from the results of Table 7, the amplitude value of pitch motion of the boat in cases 2, 6 and 9, compared to the boat without stabilizer, has decreased by 56.67%, 53.33% and 98.33%, respectively. Based on the obtained results, it can be said that for the studied boat, the appropriate depth of the hydrofoil from the heel is 10 cm, the longitudinal distance from the transom is 10 cm, and the angle of attack is 10 degrees.

6.Conclusions

In this paper, the occurrence of porpoising for a mono-hull planing craft with and without hydrofoil stabilizer were investigated. To reduce the porpoising and longitudinal instability of planing craft, a hydrofoil stabilizer with different locations were designed. First, the effect of different speeds on the occurrence of instability was investigated on bare hull. Then the effects of depth from the transom bottom, the longitudinal distance to the transom, and the angle of attack of hydrofoil stabilizer were investigated.

The analysis was done at speeds of 15, 20, 30 and 40 knots. In speed of 30 knots, the mono hull planing craft entered the stage of porpoising instability and the hydrofoil stabilizer was designed for this speed. As seen from the results, the longitudinal instability reduced by increasing depth of the hydrofoil from the bottom of the craft transom. It seems that with the increase in the depth of the hydrofoil from the transom, because it is more exposed to the incoming flow, the distribution of pressure and hydrodynamic force on it increases and also the center of pressure moves to the rear. In addition, as the depth increases, the moment arm on the boat also increases. It was also observed that the hydrofoil stabilizer has the best performance at a depth of 10 cm from the transom. It was also found from the obtained results that the longitudinal distance of the hydrofoil to transom has not significant effect on reduction of longitudinal instability. However, the proper position for the hydrofoil should be after the transom of the craft. Of course, in a boat, usually the longitudinal distance of the hydrofoil stabilizer relative to the transom is limited by the dimensions of the propeller and propulsion systems. In other words, usually the engine and propeller dimensions determine the longitudinal position of the hydrofoil stabilizer. Also, based on the obtained results, it was observed that the porposing instability was reduced by increasing the attack angle of the hydrofoil stabilizer. Of course, it should be noted that the attack angle of the hydrofoil should be lower than the stall angle. In general, it can be said from the comparison of the obtained results that by choosing a suitable hydrofoil stabilizer and choosing a suitable installation position for it, the porpoising instability of a planing mono-hull boat can be greatly reduced or eliminated.

List of Symbols

C	Chord length
B	Maximum width
T	Maximum thickness
H	Depth from the transom bottom
D	Longitudinal distance from the transom
α	Angle of attack
L_w	Wet length
U	Speed
P	Pressure
ρ	Density
ν	Kinematic viscosity
μ_t	Eddy viscosity
k	Turbulent kinetic energy
ε	Dissipation rate of turbulent kinetic energy
P_k	Production of turbulent kinetic energy

7.References

1- Savitsky, D., (1985), Planing craft. Naval Engineers Journal, Vol. 97, No.2. https://doi.org/10.1111/j.1559-3584.1985.tb03397.x

2- Ikeda Y., (2000), Stability of high speed craft. In: Vassalos D, et al., editors. Con-temporary ideas on ship stability. New York: Elsevier Science Ltd.; 2000.p. 401–9. https://dx.doi.org/10.1016/B978-008043652-4/50031-6

3- Faltinsen, O.M., (2005), Hydrodynamics of High-Speed Marine Vehicles; Cambridge University Press: Cambridge, UK. https://dx.doi.org/10.1017/CBO9780511546068

4- Celano, T., (1998), The Prediction of Porpoising Inception for Modern Planing Craft. SNAME Transactions 106, pp.269-292.

5- King D. W., Lockwood A. L., (1928). Anti-cavitation plate for outboard motors. United States Patent Office. Patent No.: 1,734,911. Nov. 5, 1929, Appl. No. 290,306.

6- Larson W., (1984). Boat stabilizer. United States Patent Office. Patent No.: 4,487,152., Appl. No. 482,401.

7- Day, J. P., Haag R. J., (1952). Planing Boat Porpoising-A Study of the Critical Boundries for a Series of Prismatic Hulls, Thesis submitted to Webb Institute of Naval Architecture, Glen Cove, Long Island, N.Y.

8- Savitsky, D., (1964), Hydrodynamic design of planing hulls. Mar. Technol. SNAME News 1964, 1, 71–95. https://doi.org/10.5957/mt1.1964.1.4.71

9- Clement, E.P., Blount, D.L., (1963), Resistance tests of a systematic series of planing hull form, Trans. SNAME 71.

10- Brown, P., (1971), An experimental and theoretical study of planing surfaces with trim flaps, Davison Laboratory report 1463, Stevens institute of Technology, Hoboken, NJ, USA.

11- Savitsky D., Brown P., (1976). Procedures for hydrodynamic evaluation of planing hulls in smooth and rough water, Marine Technology vol. 13, pp. 381-400. https://doi.org/10.5957/mt1.1976.13.4.381

12- Blount, Doald L., Codega Louis T., (1992), Dynamic stability of planing boats. Marine Technology, Vol. 29, No. 1, pp. 4-12. https://dx.doi.org/10.5957/mt1.1992.29.1.4

13- Kazemi H., Salari M., (2017), Effects of loading conditions on hydrodynamics of a hard-chine planing vessel using CFD and a dynamic model, International Journal of Maritime Technology, ijmt2017;7:11-18. https://dx.doi.org/10.18869/acadpub.ijmt.7.11

14- Xiaosheng, B., Hailong, S., Jin, Z., Yumin, S., (2019). Numerical analysis of the influence of fixed hydrofoil installation position on seakeeping of the planing craft. Appl. Ocean Res. 2019, 90, 101863. https://doi.org/10.1016/j.apor.2019.101863

15- Liru Zan, Hanbing Sun, Shijie Lu, Jin Zou, Lei Wan, (2022), Experimental Study on Porpoising of a High-speed Planing Trimaran. Journal of Marine Science Engineering, 11, 769. https://doi.org/10.3390/jmse11040769

16- McCroskey, W. J., (1987), A Critical Assessment of Wind Tunnel Results for the NACA 0012 Airfoil. NASA Technical Memorandum.

17- Sport marine technologies Inc. Products. Available: https://sesport.wpengine.com

18- ITTC., (2014). Practical Guidelines for Ship CFD Applications. Recommended procedures and guidelines section: 7.5-03-02-03 2014b.